CFD Analysis of Propeller Tip Vortex Cavitation in Ship Wake Fields

[1]Keun Woo Shin*; [2]Poul Andersen

[1]MAN Diesel & Turbo, Frederikshavn, Denmark; [2]Technical University of Denmark (DTU), Kgs.Lyngby, Denmark

Abstract

TVC on marine propellers in behind-hull conditions is a challenging problem for numerical predictions, because it is deformed in turbulent viscous interactions with hull wake, propeller-induced flows and rudder disturbance. DES is made for cavitating flows on a propeller and a rudder of a military vessel with a 3.5° shaft inclination in non-uniform hull wake. While a cavitation tunnel test shows TVC extending over the rudder, only a short extent of TVC is reproduced in DES on the initial grid. After an adaptive grid refinement based on the Q-criterion, a larger extent of TVC is simulated and the first- and second-order pressure pulses on two points above the propeller are closer to the experimental measurements. The effects of hull wake, propeller-induced flow, rudder disturbance and shaft inclination on TVC are analyzed by looking into the deformation of the helical trajectory identified by a Q-criterion iso-surface.

Keywords: tip vortex cavitation; marine propeller; CFD; DES; hull wake; adaptive grid

Introduction

Tip vortex cavitation (TVC) on marine propellers is increasingly a subject of concern in propeller design, because it is responsible for broadband hull vibration and rudder erosion in many cases [1, 2]. As the environmental impact of the underwater radiated noise from cavitating propellers is highlighted, the need for predicting TVC behavior is increased, because TVC is often the first cavitation type shown at the lowest inception speed and is propagated far downstream from the aftship. The intensity of TVC can be reduced by lowering the blade tip loading, but abrupt tip unloading can trigger erosive cloud cavitation and stable TVC can be a safe way to let sheet cavitation depart from the blade surface without violent collapse [3].

The prediction of TVC behavior in actual propeller operations behind a hull is a complex flow problem, as the helical trajectory of TVC is deformed by hull wake, propeller-induced flow and rudder interaction. Hybrid methods consisting of a viscous flow solver for the hull flow, a potential flow solver for the propeller flow and an empirical model for TVC are efficient for predicting high-order pressure pulses induced by TVC, but have limitations in taking interactive dynamics into account [4]. Extensive TVC on an open-water propeller is simulated by a viscous flow solver with a multiphase model [5], but the simulation in behind-hull conditions is still challenging due to high computational effort required for resolving tip vortex flows. In this research work, detached-eddy simulations (DES) are made for TVC on a propeller and a rudder of a military vessel with a 3.5° shaft inclination in non-uniform hull wake. A cavitation tunnel test conducted with a complete hull model at SSPA shows that TVC is extended over the rudder for about one blade revolution in the loading condition of the maximum engine power.

CFD setup

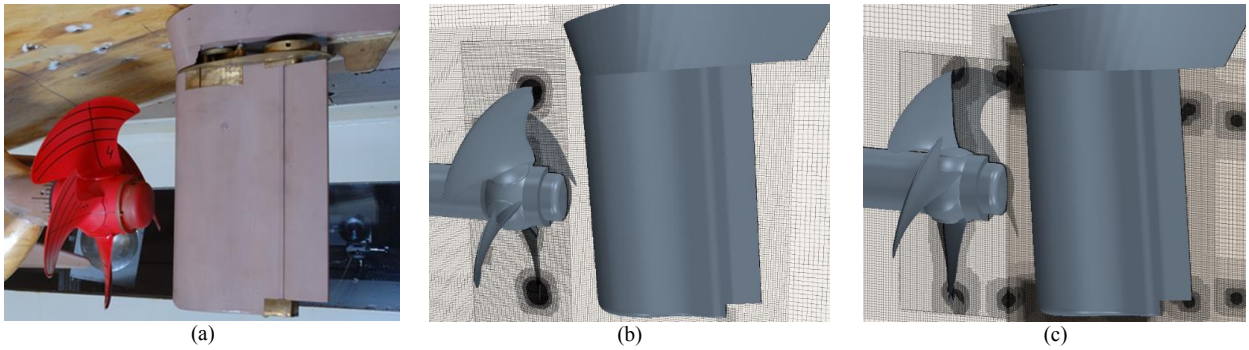

(a) (b) (c)

Figure 1. (a) Experimental setup and (b) initial & (c) refined grids of computational model

*Corresponding Author, Keun Woo Shin: keun.shin@man.eu

Downloaded from http://turbomachinery.asmedigitalcollection.asme.org/ebooks/chapter-pdf/3823048/861851_ch47.pdf by guest on 03 December 2022

The improved delayed DES solver of the commercial CFD software StarCCM+ is adopted with the curvature-corrected k-ω SST turbulence model. Cavitation is modelled by using an Eulerian multiphase approach of the volume-of-fluid method and a vapor transport equation with an interphase mass-transfer model based on the asymptotic Rayleigh-Plesset equation. Instead of including the hull model, the hull wake is modelled as a propeller inflow by using the inlet flow and momentum sources. DES results for unsteady sheet and cloud cavitation on another propeller with hull wake modeling have been validated against experimental results [6].

The propeller model is 4-bladed with a diameter of D=230 mm and a high area ratio of A_E/A_O=0.76, where A_E is the expanded blade area and A_O is the propeller disk area. Trimmed hexahedral mesh is generated around the propeller and rudder with prismatic mesh resulting mostly in a dimensionless first-cell height of y^+<2 on the wall surface in a cylindrical fluid domain. The grid is initially refined to a cell size of Δx=0.2 mm along the blade edges and at the outer-radii region around the tip. The propeller rotation is modelled by the rigid body motion and the sliding mesh in an inner cylindrical domain around the propeller.

The propeller shaft is aligned with the axis of the cylindrical domain and instead, the rudder is rotated around the blade reference line perpendicular to the ship center plane for taking into account the shaft 3.5° inclined downward at the aft end in the computational model, so that the axial component of the hull wake applied to the inlet boundary may be less disturbed on the way to the propeller plane. The radial and tangential wake components are modelled by momentum sources applied $0.6{\cdot}D$ upstream from the propeller plane. The strength of the momentum sources are adjusted by numerical tests in the same CFD setup excluding the propeller model and the velocity field on the propeller plane extracted from the final wake modeling test is compared with experimental wake measurements in figure 2. Since the hull wake is from a single-screw ship, it is symmetric with respect to the centerline.

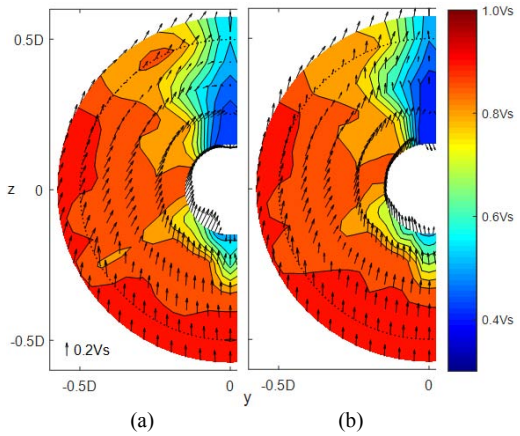

(a) (b)

Figure 2. Hull wake: (a) experimental measurement, (b) CFD modelling

An unsteady simulation is made on the initial grid starting with a time-step Δt corresponding to 6° propeller rotation per Δt and gradually reducing it to 0.5° rotation per Δt. The condition showing the largest extent of TVC in the cavitation tunnel test is considered in the simulation: ship speed V_S=4.5 m/s, propeller speed N=23.2 rps and cavitation number σ=5.42, where $\sigma=(P_\infty-P_V)/(0.5{\cdot}\rho{\cdot}V_A^2)$, P_∞ is the static pressure on the propeller shaft axis and V_A is the propeller advance speed. The propeller is on a controllable-pitch hub and the propeller pitch is increased for the maximum loading condition.

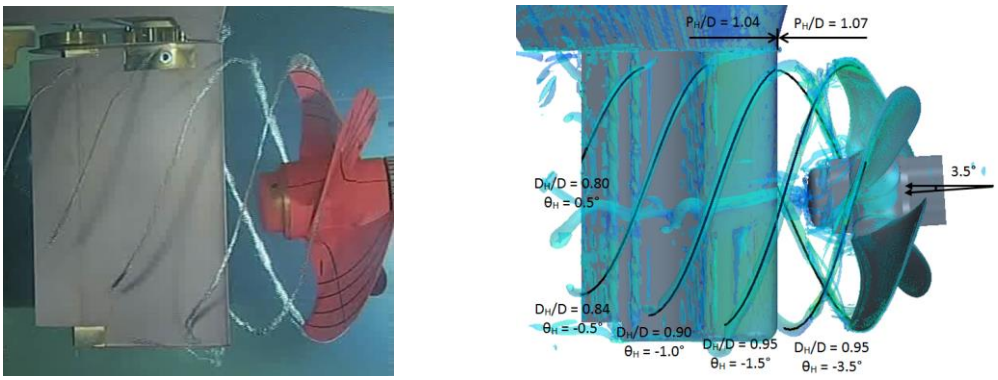

(a) (b)

Figure 3. (a) TVC in experiment and (b) iso-surface of Q-criterion=100,000 in DES with CAD helix curves

The helical trajectory of TVC identified by the iso-surface of a calibrated Q-criterion value shows a good agreement with that in the experiment until reaching the rudder. After TVC is disturbed by the rudder, the pitch P_H and diameter D_H of the helical trajectory in DES differ from those in the experiment. An overset grid is defined in a

Downloaded from http://turbomachinery.asmedigitalcollection.asme.org/ebooks/chapter-pdf/3823048/861851_ch47.pdf by guest on 03 December 2022

region over the rudder downstream from the rotating domain. As shown in figure 1(c), adaptive grid refinement of Δx=0.2 mm along the helical trajectory is applied to the overset grid region and the rotating domain. The overset grid rotates at the same speed as the propeller. Another simulation is made on the refined grid.

CFD result for TVC

In figure 4, the cavity interface visualized by the iso-surface of 10% vapor fraction in DES is compared with the experiment result. The comparison shows a good agreement in the leading-edge sheet cavitation at blade angles of φ=0 – 30°, but it is formed from more inner radii at φ=270 – 330° in DES, where φ=0° indicates the 12 o'clock blade position.

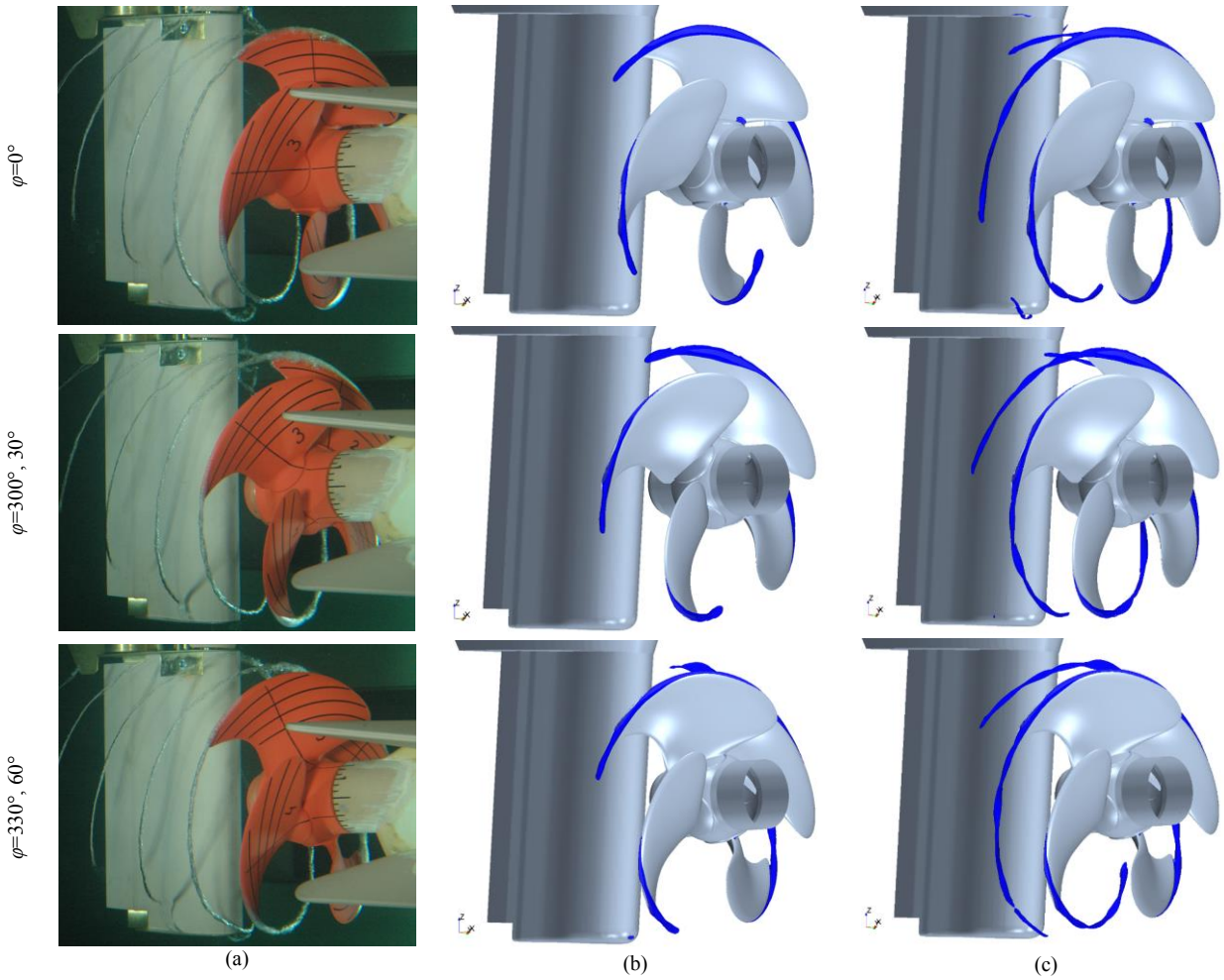

Figure 4. Cavitating flows on propeller and rudder in (a) experiment and DES on (b) initial and (c) refined grids

In the experiment, TVC is formed with a spiral structure from the roll-up of the trailing vortex sheet at the beginning and it is developed to be a concentrated vortex with a round cross section after about one quarter revolution. DES on the initial grid shows only a short extent of TVC with a round cross section, because the fine vortex core is not sufficiently resolved. After the grid refinement, TVC is more extended with a pronounced spiral structure, but it is still shorter than in the experiment. As TVC is distorted by the rudder disturbance, some parts of TVC can deviate from the refined grid region and so TVC from the blade at φ=300 – 330° is more extended than at φ=0 – 30°, because the grid refinement is made once for a certain momentary trajectory. The grid refinement to Δx=0.2 mm may not be enough to resolve the concentrated TVC core tapering downstream.

In figure 3(b), the deformation of TVC is analyzed by fitting CAD helix curves on the Q-criterion iso-surface. The initial pitch ratio of P_H/D=1.07 is reduced to P_H/D=1.04 by the rudder disturbance after a quarter of a revolution,

Downloaded from http://turbomachinery.asmedigitalcollection.asme.org/ebooks/chapter-pdf/3823048/861851_ch47.pdf by guest on 03 December 2022

which is contrasted to a 3% increase of the initial pitch further downstream shown in experiments on other propellers in uniform inflow with a straight shaft and no appendage [7]. P_H in the open-water experiments is about 5% higher than estimations from the actuator disc formula $P_H/D=J\cdot(1+(1+C_{Th})^{0.5})/2$, where J is the advance coefficient and C_{Th} is the thrust loading coefficient. If there is no rudder, the downstream pitch can be increased to $P_H/D=1.10$, which is 11% higher than $P_H/D=0.99$ from the actuator disc formula, because the propeller loading considered in DES corresponds to the maximum engine power, which is 1.67 times higher than the engine power of the design condition.

The initial diameter ratio of $D_H/D=0.95$ is gradually decreased to $D_H/D=0.8$ due to the radially inward propeller-induced flow. It is smaller than $D_H/D=0.83$ in the open-water experiments [7] due to the stronger flow acceleration in the high loading condition. The contraction of TVC is larger than the slipstream diameter reduction estimated to be about 4% by a formula derived from potential-flow calculations without considering rudder effects [8]. The angle θ_H of the progressing direction is 3.5° downwards along the shaft axis for an initial quarter of a revolution and it is gradually tilted upwards to $\theta_H=0.5°$ by the upward flow of the hull wake.

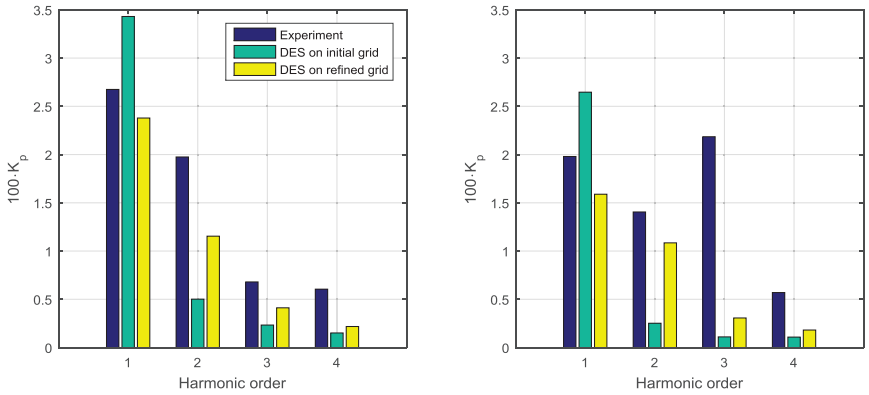

Figure 5. Pressure pulses on two points above the propeller $0.51\cdot R$ downstream from the propeller plane and $0.51\cdot R$ to (a) port and (b) starboard sides from the centerline

In figure 5, dimensionless pressure pulses K_P on two points above the propeller at harmonics of the blade passing frequency are compared between the experiment and DES, where $K_P=\acute{P}/(\rho\cdot N^2\cdot D^2)$ and $\acute{P}$ is the pressure amplitude. The two points are located $0.51\cdot R$ from the centerline to both sides, $0.51\cdot R$ downstream from the propeller plane and $1.58\cdot R$ above the shaft axis. While the experimental measurements are made on the hull surface, the pressure is probed in the middle of the fluid domain without a wall boundary in DES and so the pressure pulse in DES is increased by a multiplication factor of 2 as per [8].

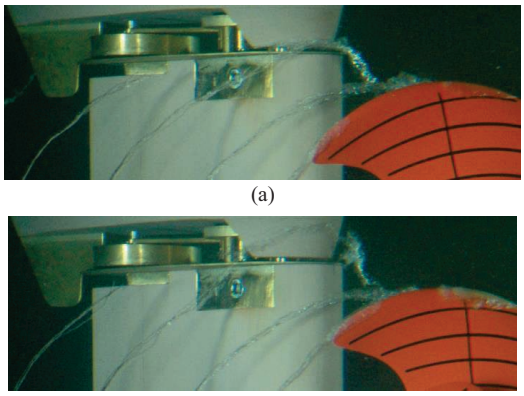

Figure 6. Collapsing of TVC at the gap between the rudder and the headbox in experiment at (a) φ=350° and (b) φ=0°

After the grid refinement, the first- and second-order pressure pulses are closer to the experimental measurements. Although the third- and fourth-order pressure pulses are increased in DES on the refined grid, these are still lower than the experimental ones. In the experiment, the third-order pressure pulse is higher than the first- and second-order ones on the starboard-side point (See figure 5 (b)), which may be related to the TVC collapse at the gap between the rudder and the headbox shown in figure 6. As TVC in DES is not extended to the rudder, the high-order pressure pulses are underestimated.

Downloaded from http://turbomachinery.asmedigitalcollection.asme.org/ebooks/chapter-pdf/3823048/861851_ch47.pdf by guest on 03 December 2022

Conclusion

The adaptive grid refinement based on the Q-criterion with the overset grid over the rudder is effective in resolving TVC in DES. As TVC is better resolved by the grid refinement, the first- and second-order pressure pulses on two points above the propeller are closer to the experimental result. But the underestimation of high-order pressure pulses is significant, probably because the TVC collapse at the rudder headbox is not reproduced well. Repetitive grid refinements to smaller cell sizes of $\Delta x \leq 0.2$ mm may improve the accuracy to reproduce a larger extent of TVC.

The vortex flow visualization in DES is a useful tool for analyzing the deformed trajectory of TVC in the non-uniform hull wake field. The pitch of the TVC trajectory is reduced by the rudder disturbance in contrast with the pitch increase downstream in the open-water condition. The initial pitch is larger and the downstream radius is smaller due to the higher propeller loading than for moderately loaded propellers. The upward tilt of the TVC progress is pronounced by the upward flow of the hull wake and the downward inclination of the shaft axis.

Acknowledgements

The authors would like to express their gratitude for the support granted by the Danish Maritime Fund (Den Danske Maritime Fond).

References

[1] van Terwisga, T., Fitzsimmons, P. A., Ziru, L. and Foeth, E. J. (2009) *Proc. CAV2009* (Ann Arbor, MI, USA)
[2] Arndt, R., Pennings, P., Bosschers, J. and van Terwisga, T. (2015) *Interface Focus* 5: 20150025
[3] Shin, K. W. and Andersen, P. (2015) *Proc. CAV2015* (Lausanne, Switzeland)
[4] Berger, S., Gosda, R., Scharf, M., Klose, R., Greitsch, L. and Abdel-Maksoud, M. (2016) *Proc. 31st Symp. on Naval Hydrodynamics* (Monterey, CA, USA)
[5] Viitanen, V. M., Hynninen, A., Lubke, L., Klose, R., Tanttari, J., Sipila, T. and Siikonen, T. (2017) *Proc. SMP'17* (Espoo, Finland)
[6] Shin, K. W., Regener, P. B. and Andersen, P. (2015) *Proc. SMP'15* (Austin, TX, USA)
[7] Kerwin, J. E. (1976) *A deformed wake model for marine propellers* (Cambridge, MA, USA: MIT)
[8] Bertram, V. (2000) *Practical ship hydrodynamics* (Woburn, MA, USA: Butterworth-Heinemann)
[9] Hasuike, N., Yamasaki, S. and Ando, J. (2011) *Proc. MARINE 2011* (Lisbon, Portugal)

Downloaded from http://turbomachinery.asmedigitalcollection.asme.org/ebooks/chapter-pdf/3823048/861851_ch47.pdf by guest on 03 December 2022

© 2018 ASME